Proceedings of the 2005 IEEE
International Conference on Robotics and Automation
Barcelona, Spain, April 2005

Concept Development and Design of a Spherical Wheel Motor (SWM)

Kok-Meng Lee*, Hungsun Son, and Jeffry Joni
Georgia Institute of Technology
The George W. Woodruff School of Mechanical Engineering
Atlanta, GA 30332-0405
Corresponding author: Email: kokmeng.lee@me.gatech.edu; Phone: +1(404)894-7402; Fax: +1(404)894-9342

Abstract: **This paper presents the design concept, models, and open-loop control of a particular form of a variable-reluctance spherical motor (VRSM), referred here as a spherical wheel motor (SWM). Unlike existing spherical motors where design focuses have been on controlling the three degrees of freedom (DOF) angular displacements, the SWM offers a means to control the orientation of a continuously rotating shaft in an open-loop (OL) fashion. We provide a formula for deriving different switching sequences (full step and fractional step) for a specified current magnitude and pole configurations. The concept feasibility of an OL controlled SWM has been experimentally demonstrated on a prototype that has 8 rotor permanent-magnet (PM) pole-pairs and 10 stator electromagnet (EM) pole-pairs.**

Keywords: **Brushless motor, Stepper, Spherical motor, ball-joint-like actuator, wrist actuator.**

I. INTRODUCTION

Many mobile vehicles such as car wheels [1], propellers for boats, helicopter or underwater vehicle, gyroscopes, and machine tools require orientation control of the rotating shaft. The growing interests in fuel-cell technology and low-cost electric vehicles have motivated a number of researchers to develop alternative design of wheel motors [2]. Existing designs are typically single-axis devices; thus, orientation control of their rotating shafts must be manipulated by an external mechanism. These multi-axe spinners are generally bulky, slow in dynamic response, and lack of dexterity in negotiating the orientation of the rotating shaft.

This paper presents an alternative design built upon the concept of a VRSM previously developed at Georgia Tech [3]. The SWM, much like the VRSM capable of offering three-DOF in a single joint, is essentially a ball-joint-like, brushless, direct-drive actuator. However, unlike VRSM where the focus has been on controlling the three-DOF angular displacements, the SWM discussed here offers a means to control in open-loop (OL) the orientation of its rotating shaft with a single spherical joint.

Spherical motors take a number of forms which include the induction motors [4] [5], the direct-current motors [6] [7] [8], the stepper [9] [10], the variable-reluctance spherical motors [3] [11], the ultrasonic motor [12] and also in [13]. Compared with its counterparts, the spherical stepper has a relatively large range of motion, possesses isotropic properties in motion, and is relatively simple and compact in design. In addition, it can operate in open-loop and thus provides an incentive for further development as a SWM.

The basic concept of a spherical stepper was originally proposed by [9]. Reference [10] studied the method to place the rotor poles for stepping motion on a structure similar to that suggested in [9]. The dynamic model of a particular VRSM can be found in [3], where the torque model is a quadratic function of the current inputs to the stator coils. A similar study can also be found in [11], in which they derived the torque vector and the back electromotive forces in closed form based on an analytical magnetic field distribution. More recently, the interest to derive a closed-form solution to the inverse torque model has led [14] to design a VRSM that has a linear torque-current relationship.

Most of research on spherical motors has focused on developing alternative design concepts, torque models, and more recently on developing non-contact sensors for measuring three-DOF orientation for feedback control. These existing spherical motors (motivated by the advance in robotic technology) have pre-dominantly been designed for wrist like motions; the primary interest has been the control of three-DOF orientation displacements. We investigate here the feasibility of designing a VRSM for applications (such as transportation and machine tools) that require the dexterous orientation control of a rotating shaft.

This paper focuses on concept development and design of a SWM. Specifically, this paper offers the following:

1. We present the design of a SWM and highlight the structural differences between a VRSM and a SWM.

2. The torque and dynamic models, which provide a means to illustrate the operational principle and to analyse the performance of a SWM, are given. The models will also serve as a cost-effective basis to streamline the design process and reduce development time of a SWM prototype.

3. We describe the method to control the orientation of the SWM in open-loop while allowing the rotor to spin continuously. Specifically, we provide a formula for deriving different switching sequences for a specified current magnitude and pole configurations. We illustrate in detail the switching method for a SWM that has 8 rotor PM pole-pairs and 10 stator EM pole-pairs.

4. Finally, we demonstrate experimentally the concept feasibility of a SWM prototype with 10 EM pole-pairs modified using an existing VRSM [3].

II. DESIGN OVERVIEW OF THE SWM

Reference [14] derived a general torque model for a VRSM based the principle of variable-reluctance; the torque generated electromagnetically has the form:

$$T_k = \frac{1}{2}\mathbf{u}_s^T \frac{\partial[L_{ss}]}{\partial\theta_k}\mathbf{u}_s + \mathbf{u}_r^T \frac{\partial[L_{rs}]}{\partial\theta_k}\mathbf{u}_s + \frac{1}{2}\mathbf{u}_r^T \frac{\partial[L_{rr}]}{\partial\theta_k}\mathbf{u}_r \qquad (1)$$

where θ is the angular displacement; k (= 1, 2, and 3) denotes the x, y and z components; the subscripts r and s denote the rotor and stator respectively; $\mathbf{u}$ is the current vector; $[L_{ss}]$ and $[L_{rr}]$ are the self inductance sub-matrices of the stator and rotor respectively; and $[L_{sr}] = [L_{rs}]^T$ is the mutual inductance sub-matrix.

II.1 CAD Model Illustrating the Design Concept

Fig. 1 shows a CAD illustration of the SWM that consists of rotor, stator, and sensor subassemblies. This has been a modified design of the VRSM in [3] but has the following differences:

1. The SWM uses permanent magnets (PM's) to replace the irons as rotor poles, and aluminum to replace the iron cores on which the wires of the stator electromagnets are wound. Thus, unlike the torque model of a VRSM [3] which is characterized by the first term of (1), we consider here a design where the torque acting on the rotor can be approximated as a linear combination of stator currents:

$$T_k \approx \mathbf{u}_r^T \frac{\partial[L_{rs}]}{\partial\theta_k}\mathbf{u}_s = [K(\mathbf{q})]\mathbf{u}_s \qquad (2)$$

where $\mathbf{q} = [\psi \ \theta \ \phi]^T$ is a vector of ZYZ angles. For this design, the third term on the right side of (1) is zero since no torque is generated corresponding to zero current and with non-ferromagnetic cores, the self-inductance $[L_{ss}]$ of the electromagnets is very small such that the second term in (1) dominates.
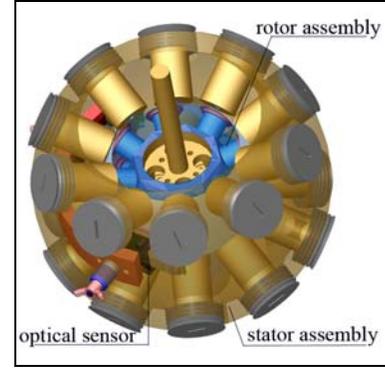
2. Unlike the VRSM where the PM's and EM's are placed on locations following the vertices of a regular polygon, equally-spaced magnetic poles are placed on layers of circular planes for a SWM as illustrated in Fig. 2, where R is the radius of the spherical rotor; and δ is the angle between the two adjacent poles on a circular plane. The SWM has m_r pairs of rotor PM's and m_s pairs of stator EM's; both m_r and m_s are even integers. The magnetization axes of these PM's or EM's, which pass radially through the motor center, can be characterized mathematically by a vector. The magnetization axis of a rotor pole-pair, in the rotor frame xyz, is given by (3):

$$\mathbf{r}_i = (-1)^i \left[\cos\gamma_r \cos(i-1)\delta_r \quad \cos\gamma_r \sin(i-1)\delta_r \quad \sin\gamma_r \right]^T \qquad (3)$$
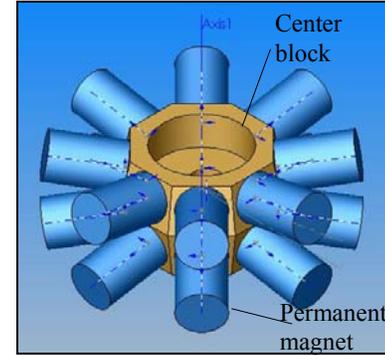
where i= 1, 2,..., m_r. Similarly, the direction of the EM's in the stator frame XYZ is given by (4):

$$\mathbf{s}_j = \left[\cos\gamma_s \cos(j-1)\delta_s \quad \cos\gamma_s \sin(j-1)\delta_s \quad \sin\gamma_s \right]^T \qquad (4)$$
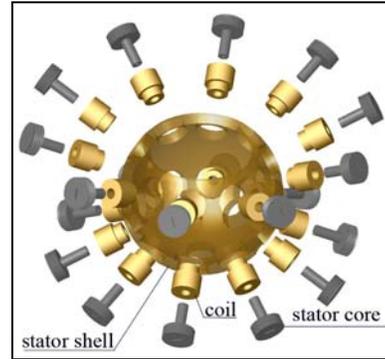
where j= 1, 2,..., m_s.

(a) SWM

(b) Rotor assembly

(c) Exploded view of the stator assembly
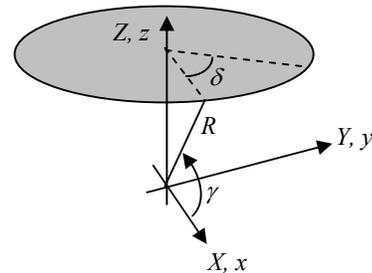
Fig. 1 CAD Model of a SWM

Fig. 2 Circular plane of pole location

The resolution of a stepping motor depends on the number of rotor pole pairs, the number of stator EM pole-pairs and the drive mode (full or fractional step). As will be

shown in Section III, δ_r and δ_s define the step size of a switching sequence.

II.2 Torque Model

Since the magnetic circuit is linear, the torque generated by the interaction of jth stator pole pair and m_r rotor pole pairs can be evaluated as follows:

$$\widehat{\mathbf{T}}_{js} = \sum_{k=1}^{m_r} \hat{f}(\varphi_{jk}) \frac{\mathbf{s}_j \times \mathbf{r}_k}{\left\| \mathbf{s}_j \times \mathbf{r}_k \right\|} u_j \tag{5}$$

where φ_{jk} is the separation angle between the jth stator pole pair and the kth rotor pole-pair; and $\hat{f}(\varphi_{jk})$ is an approximation of the torque constant derived from the computed data using the finite-element (FE) method [15]. The method for deriving $\hat{f}(\varphi_{jk})$ from ANSYS [16], an off-the-shelf FE analysis package, has been given in our earlier paper [14]. ANSYS is used to solve for the magnetic field distribution. However since the ANSYS FE package does not provide torque as an output, a macro was written to compute the torque generated by summing the cross products of the elemental force:

$$\mathbf{T} = -\int_V \mathbf{a} \times (\mathbf{J} \times \mathbf{B}) dV \tag{6}$$

where $(\mathbf{J} \times \mathbf{B})$ is the Lorentz force; and $\mathbf{a}$ represents the moment arm perpendicular to the axis of rotation and directed to the point where the force is computed.

As shown in (3), the rotor PM pole-pairs are designed such that adjacent PM's have opposite polarities. The FE analysis is performed for two opposite interaction pair of the rotor PM pole-pair and stator EM pole-pair with parameters given in Table 1. Fig. 3 shows the geometric model used in ANSYS for the SWM, where the centre block and the stator shell are made of iron so that a closed magnetic loop among the rotor pole-pair, the centre block, the stator pole-pair, and returned through the stator shell.

Table 1 Stator and Rotor Pole Pair

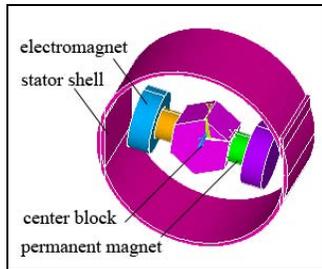|	
Stator EM pole	OD = 0.75 in, 1050 turns
Coil wire and resistance	29 AWG, 6.46 Ohms
Current (2 EM's in series)	4 Amperes
Rotor radius	76.2 mm (3 inches)
Cylindrical PM	OD=L=12.5mm (0.5in)
Air-gap between EM & PM	0.762mm (0.03in)

Fig. 3 ANSYS model for FE analysis

The computed torques (generated by the interaction between the stator EM pole-pair and the rotor PM pole-pair) are plotted in Fig. 4 as a function of the separation angle between the two magnetization axes. Fig. 4 also compares the torques generated by two different structures; namely, ferrous and non-ferrous materials for the stator shell and the rotor centre-block. The companion shows that closed magnetic path guided by the ferrous material could significantly increase the maximum torque as much as 67%. An approximated torque function is derived from Fig. 4:

$$\hat{f}(\varphi_{jk}) = \sum_{i=0}^{4} a_i \varphi_{jk}^i \tag{7}$$

The estimation coefficients a_i in (7) are determined to minimize the estimation error $\left\| f(\varphi_{jk}) - \hat{f}(\varphi_{jk}) \right\|^2$; and n is the order of the estimation function. These coefficients are $a_0 = 0.04329$; $a_1 = -0.00486$; $a_2 = 0.00349$; $a_3 = -1.741\text{e-}004$; and $a_4 = 2.323\text{e-}006$.
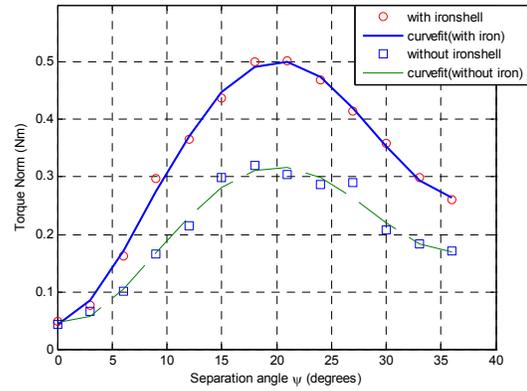

Fig. 4 Effect of magnetic path on the torque model

II. 3 Dynamic Model

To provide a means to predict the dynamic performance, we derive the rotor dynamics for an axially symmetric body about the centre O:

$$[\mathbf{M}]\ddot{q} + \mathbf{C}(\dot{q}, q) = \mathbf{Q} \tag{8}$$

where

$$[M] = \begin{bmatrix} (I_a - I_t)\cos^2\theta + I_t & 0 & I_a\cos\theta \\ 0 & I_t & 0 \\ I_a\cos\theta & 0 & I_a \end{bmatrix} \tag{8a}$$

$$C(\dot{q}, q) = \begin{bmatrix} 2(I_t - I_a)\sin\theta\cos\theta\dot{\psi}\dot{\theta} - I_a\sin\theta\dot{\theta}\dot{\phi} \\ (I_a - I_t)\sin\theta\cos\theta\dot{\psi}^2 + I_a\sin\theta\dot{\psi}\dot{\phi} \\ -I_a\sin\theta\dot{\psi}\dot{\theta} \end{bmatrix} \tag{8b}$$

and

$$\mathbf{Q} = \begin{bmatrix} -T_1\sin\theta\cos\phi + T_2\sin\theta\sin\phi + T_3\cos\theta \\ mgl\sin\theta + T_1\sin\phi + T_2\cos\phi \\ T_3 \end{bmatrix} \tag{9}$$

where $I_a = I_{zz}$ and $I_t = I_{xx} = I_{yy}$; and $\vec{r} = l\vec{k}$. In (9), the torque components (T_1, T_2, T_3) are applied about the x, y and z axes of the rotor frame. Since the stator currents are

3654

applied to generate the torques about *X, Z* about *z* axes as defined in Fig. 5, we relate (T_1, T_2, T_3) to $(T_\alpha, T_\beta, T_\phi)$ using the transformation given in (10):

$$[\mathbf{T}]_{123} = R(\phi, \theta, \psi)[\mathbf{T}]_{XYZ} \qquad (10)$$

where

$$[\mathbf{T}]_{XYZ} = \sum_{j=1}^{m_s} \sum_{k=1}^{m_r} \hat{f}(\varphi_{jk}) \frac{\mathbf{s}_j \times \mathbf{r}_k}{\|\mathbf{s}_j \times \mathbf{r}_k\|} u_j$$

$$R(\phi, \theta, \psi) = \begin{bmatrix} C_\phi C_\theta C_\psi - S_\phi S_\psi & C_\phi C_\theta S_\psi + S_\phi C_\psi & -C_\phi S_\theta \\ -S_\phi C_\theta C_\psi - C_\phi S_\psi & -S_\phi C_\theta S_\psi + C_\phi C_\psi & S_\phi S_\theta \\ S_\theta C_\psi & S_\theta S_\psi & C_\theta \end{bmatrix}$$

III. OPEN-LOOP CONTROL OF A SWM

The SWM offers the ability to spin continuously (much like a brushless DC motor) while the shaft can be tilted arbitrarily from the Z-axis defined in the stator reference frame XYZ in Fig. 5.
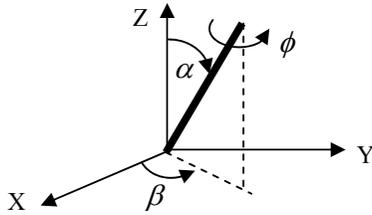

Fig. 5 Stator reference frame

The motor is designed to follow the linear relationship suggested by (2). The current input vector $\mathbf{u}(\in \mathfrak{R}^{10 \times 1})$ can be expressed as a linear combination of three terms:

$$\mathbf{u} = \left([\mathbf{I}] + [\mathbf{u}_\alpha] + [\mathbf{u}_\beta] \right) \mathbf{u}_\phi \qquad (11)$$

where $\mathbf{u}_\phi (\in \mathfrak{R}^{10 \times 1})$ is a vector governing the current components responsible for the spin motion about the rotational axis of the shaft; $[\mathbf{I}]$ is a unit matrix; $[\mathbf{u}_\alpha]$ is a portion of the currents added the α rotation; and similarly $[\mathbf{u}_\beta]$ is a portion of the currents for the β rotation.

A switching controller has been designed to illustrate the operation of a SWM that uses 10 EM pole-pairs and 8 PM pole-pairs; $m_r=8$, $m_s=10$, $\delta_r=45°$ and $\delta_s=36°$. The EM pole-pairs are divided into a multiple of identical phases because of the symmetry; the number of coils in a phase can be determined from the least common multiplier (LCM) of δr and δs. For example, there are two (or 360° divided by the LCM of δr and δs) phases for the 10EM-8PM configuration. Five different controllers $(n=1,...,m_s/2=5)$ based on the multiple of 9° ($\delta_r - \delta_s =9°$, 18°, 27°, 36°, and $\delta_r=45°$) can be designed to maintain a constant spinning rate. To facilitate discussions on effects of step size on controller design, we define the Sequence Number S_N mathematically as follows:

$$S_N = nj - (n-1) \qquad \text{where } j=1,...,m_s. \qquad (12)$$

The controller uses S_N to specify the switching sequence of the EM pole pairs as illustrated in Table 2. The open-loop control begins with the initiation of the SWM; the Z- and z-

axes are coincided and the EM pole-pairs #1 and #6 are aligned with two diametrically opposite rotor pole-pairs as shown in the illustrative plan view in Table 2. Five types of switching sequences for spinning at a constant rate are also given in Table 2, where 5 of the 10 stator EM pole-pairs (for one phase) are listed since the remaining five pole-pairs (6-10) are identical to (1-5) due to the geometrical symmetry. For example, a controller based on a 9°-step sequence would repeat the sequence number from 1 to 10 in controlling the current inputs to the EM pole-pairs, while the controller designed for a step size of δ_r=45°would repeat S_N=1 and S_N= 6.

Table 2: Stator EM Switching Sequence (9° interval)

| S_N | EM pole-pair |
	1	2	3	4	5
1	N	S	N	S	N
2	N	S	N	S	S
3	N	S	N	N	S
4	N	S	S	N	S
5	N	N	S	N	S
6	S	N	S	N	S
7	S	N	S	N	N
8	S	N	S	S	N
9	S	N	N	S	N
10	S	S	N	S	N

Fig. 6 Plan view of coil layout

Five types of switching sequences

n	Step	Switching sequence $S_N = nj - (n-1)$
1	9°	$S_N = j = 1, 2,..., 10, 1, 2,..., 10,1\,2...$
2	18°	$S_N = 2j-1 = 1, 3,..., 9,1,3,...,9,1,3...$
3	27°	$S_N = 3j-2 = 1, 4,7,1,4,7,1,4...$
4	36°	$S_N = 4j-3 = 1, 5, 9, 1, 5, 9, 1, 5,...$
5	45°	$S_N = 3j-2 = 1, 6, 1, 6,1,6,1...$

We illustrate as an example an OL switching controller based on a 45°-step sequence, which follows (13):

$$u_j = f_0 \, \mathrm{sgn}(\sin \omega_s t)|u_m|\left\{ 1 + f_1(\alpha)\cos\left[j\delta_s + f_2(\beta) \right] \right\} \qquad (13)$$

where $j = 1, 2, ...,10$;

$$f_0 = \begin{cases} (-1)^j & j=1,...,5 \\ (-1)^{j+1} & j=6,...,10 \end{cases} \quad ; \quad \mathrm{sgn}(x) = \begin{cases} 1 & if \ x > 0 \\ 0 & if \ x = 0 \\ -1 & if \ x < 0 \end{cases}$$

In (13), the scalar $f_0 \, \mathrm{sgn}(\sin \omega_s t)|u_m| = u_{\phi j}$ is a square wave with frequency ω_s and magnitude $|u_m|$. Since four cycles of current inputs are required for each revolution, the spin-rate of the rotating shaft (in rpm) is equal to $30\pi\omega_s$. The functions $f_1(\alpha)$ and $f_2(\beta)$ that govern the shaft orientation (or α and β respectively) are given by changing the current vector through

$$f_1(\alpha) = \alpha / \varphi_0 \qquad (13a)$$

and

$$f_2(\beta) = \delta_s \beta \qquad (13b)$$

where φ_0 is the initial separation angle between the stator pole-pair #1 and its adjacent rotor pole-pair in the XZ plane.

IV. EXPERIMENTAL RESULTS

We modified an existing VRSM [3] to examine the concept feasibility of a SWM using open-loop control. The

3655

setup consists of 20 stator coils (or two layers of 10 coils) and 16 permanent magnets as rotor poles (or two layers of 8 poles) as shown in Figs. 7(a) and 7(b) respectively. The EM's are wired in pairs so that two diametrically opposite interacting pair of the rotor poles and stator coils would result in a common torque as in Fig. 4. The values of the parameters are given in Tables 1 and 3.
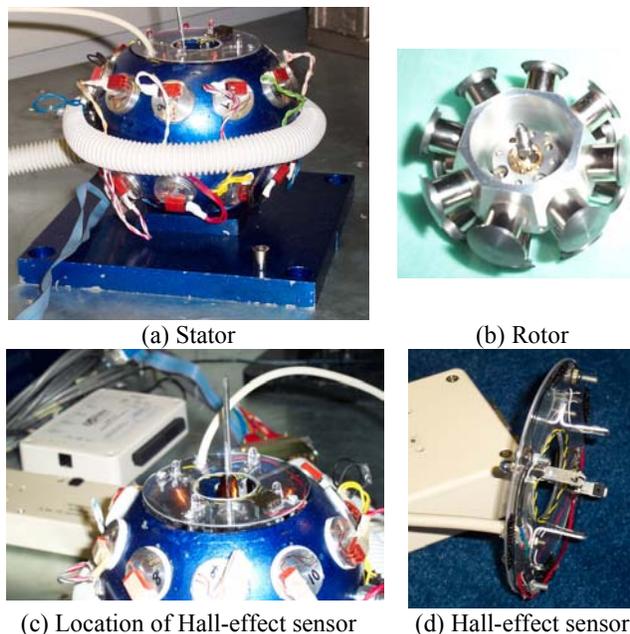

<div align="center">(a) Stator   (b) Rotor</div>

<div align="center">(c) Location of Hall-effect sensor   (d) Hall-effect sensor</div>

<div align="center">Fig. 7: SWM Prototype (a modified VRSM)</div>

Table 3: Values used in the setup

Rotor radius	76.2 mm (3 inches)
Offset of mass centre	$\bar{r} = 0$
M. of Inertia, (kg-m^2)	$I_a = 6.0576\text{e-}005$; $I_t = 3.8628\text{e-}005$
Stator EM's	20 (2 layers of 10)
Magnetization	$\gamma_s = 26°$; $\delta_s = 36°$
Current per pole-pair	$u_m = 0.3$ Ampere
Rotor PM's	16 (2 layers of 8)
Magnetization	$\gamma_r = 20°$; $\delta_r = 45°$

Other differences between the SWM and the VRSM [3] are the following: (1) we replaced the three single-axis encoders by four Hall-effect sensors as shown in Figs. 7(c) and 7(d). This eliminates the mechanical guides and thus the associated inertias and friction. (2) The transfer bearings are replaced by a spherical rolling joint [17] shown in Fig. 7(b). The exploded view in Fig. 8 illustrates the assembly of the rotor that consists of a centre block, a rotor shell of non-ferrous material, and the PM's. On the centre block, two layers of PM's are attached as shown in Fig. 7(b). The lower part of the centre block serves as a base on which the spherical rolling joint is mounted, while the top section is a shaft holder where the shaft can be held.

An open-loop controller designed for the 10-phase (10 stator EM pole-pairs) structure using a 45°-step resolution is demonstrated experimentally in the following discussion, for which only two sequence types (S_N=1 and S_N= 6) are used as illustrated in Table 2. The open-loop control commands are as follows:

Initialization: Four stator pole-pairs (#1, #3, #4, and #6) are given specified currents with same polarity to attract the nearest pairs of rotor magnets such that the shaft aligns with the Z-axis of the stator frame.

Constant spin at 340 rpm:
   The Sequence Number S_N (1, 6) are given the current $u_m = 0.3$A; ω_s =35.6rad/s, $f_0 = 1$, $f_1(\alpha) = f_2(\beta) = 0$

Spin at 340 rpm while the shaft is tilted to α=6°:
   $f_1(\alpha) = 6 / 6.565$ and $f_2(\beta) = 0$
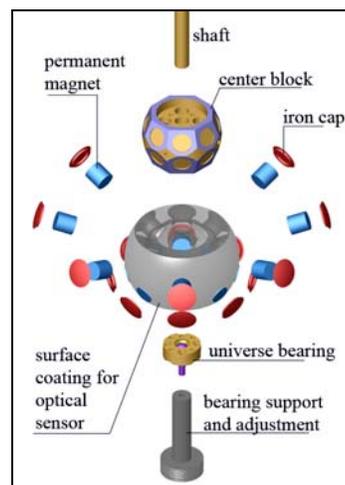

<div align="center">Fig. 8 Exploded view illustrating the rotor assembly</div>

The results are given in Figs. 9, 10, and 11. Fig. 9 shows that the process starts from an initially random inclination, moves to the pre-determined upright position ($\alpha=\beta=0$, ϕ=90°), and spins to 340rpm. Fig. 10 show that the experimentally measured spin-rate (in volts) at steady-state well matches the desired values. Fig. 11 compares the simulated and experimental responses to a step change in α $=6°$ while the rotor spin at 340rpm about its z--axis. As shown in Fig. 11, the step command on the α motion has some coupling effects on the β motion. However, the transient response of the β motion eventually decays to a small steady sate error. Similar results can also be demonstrated for the β motion. These results demonstrate that the SWM functions as a 3-DOF stepper that can be operated in open-loop. The open-loop control shown above, however, does not take into account the dynamics of the motor, which could result in a significant lag during the transient. This phase lag could cause the system to become unstable. It is expected that these dynamic effects can be compensated using feedback control.

V. CONCLUSIONS

We presented the design concept, model and open-loop control of a SWM, and showed how the orientation of the SWM can be open-loop controlled while its rotor spins continuously. We have also discussed the effects of step size resolution on the design of the OL controller, and illustrate in detail the switching method for a SWM that has 8 rotor PM pole-pairs and 10 stator EM pole-pairs.

The design concept of the SWM has been experimentally demonstrated at no load. Preliminary results

presented here did not take into account the motor and load dynamics, which could result in significant phase lag during transient. This phase lag could significantly affect the motor stability. It is expected that these dynamic effects can be compensated using feedback control, a research topic being investigated.
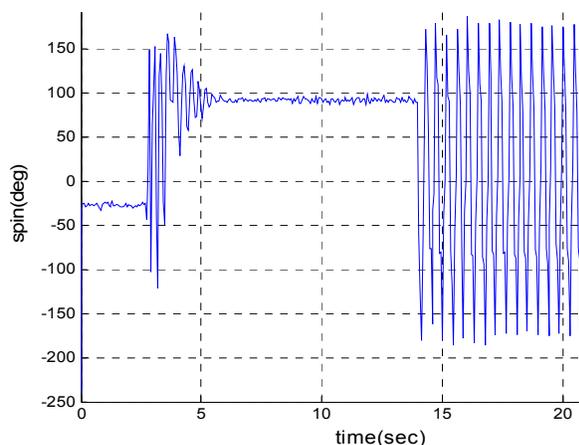

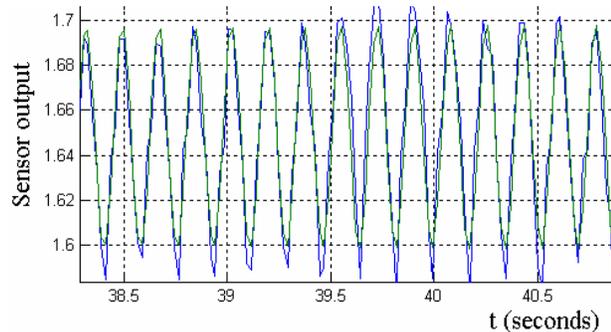Fig. 9 Initiation and transient to constant spin of 340rpm

Fig. 10 Steady-state spin of 340rpm at $\alpha = \beta = 0$
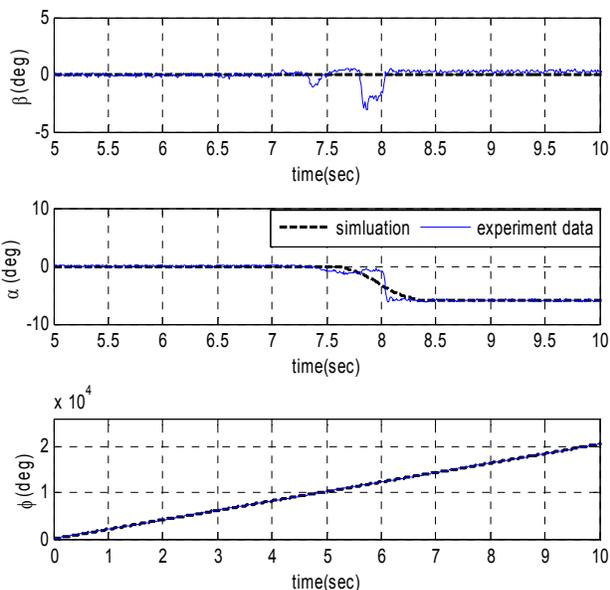Solid green line: desired; Dashed blue line: measurement

Fig. 11 Step change in α while spinning at 340rpm

REFERENCES

[1] Clarke, W., 2002, "Mercedes-Benz F-400 Carving," edmunds.com.

[2] Peter, J. 2004 "The Wave of the Future?" *Automotive Industries*, January.

[3] Lee, K-M., R. Roth, and Z. Zhou, 1996, "Dynamic Modeling and Control of a Ball-joint-like VR Spherical Motor," ASME *J. of Dyn. Sys. Meas. and Control,* vol. 118, no. 1, pp. 29-40, March.

[4] Vachtesevanos, G.J., K. Davey, & K.M. Lee, 1987, "Development of a Novel Intelligent Robotic Manipulator," IEEE *Control Systems Magazine*, June.

[5] Foggia, A., E. Oliver & F. Chappuis , 1988, "New Three DOF Electromagnetic Actuator," *Conference Record – IAS Annual Meeting*, Vol. 35, New York.

[6] Hollis, R.L., A.P. Allan, & S. Salcudean, 1987, "A Six Degree-of-freedom Magnetically Levitated Variable Compliance Fine Motion Wrist," Fourth Int'l Symp. on Robotics Research, Santa Cruz.

[7] Kaneko, K., I. Yamada, & K. Itao, 1988, "A Spherical DC Servo Motor with Three Degrees of Freedom," *ASM Dyn. Sys. & Con. Div.*, Vol. 11, p. 433.

[8] Neto, L., R. Mendes, & D. A. Andrade, 1995, "Spherical Motor- a 3D Position Servo," *Proc. IEEE Conf. on Electrical Machines and Drives*, 11-13 Sept., pp. 227-231.

[9] Lee, K-M. & C.-K. Kwan, 1991, "Design Concept Development of a Spherical Stepper for Robotic Applications," *IEEE T-Robotics and Automation,* Vol. 7, no.1, pp. 175-180, February 1.

[10] Chirikjian, G. S*., & D. Stein, 1999, "Kinematic Design and Commutation of a Spherical Stepper Motor," *IEEE/ASME T-Mechatronics* Vol. 4, No. 4, Dec.

[11] Wang, J., G. Jewel, & D Howe, 2003, "Design and Control of a Novel Spherical Permanent Magnet Actuator with Three DOF," *IEEE/ASME Trans. on Mechatronics,* Vol. 8, No. 4, Dec., 457-467.

[12] Shigeki, T., Osamu, M., & Guoqiang, Z., *1996* "Development of New Generation Spherical Ultrasonic Motor," *ICRA96*, pp. 2871-2876.

[13] Yang, C. I. & Y. S. Baek, 1999, "Design and Control of the 3 DOF Actuator by Controlling the Electromagnetic Force," *IEEE/ASME T- Mechatronics*, Vol. 35, No. 5, Sept.

[14] Lee, K.-M. R. A. Sosseh & Z. Wei, 2004, "Effects of the Torque Model on the Control of a VR Spherical Motor," *IFAC J. of Contr. Eng. Practice,* Vol 12/11 pp 1437-1449.

[15] Seminar notes, 1987, "ANSYS: Magnetic Seminar," Swanson Analysis Systems, Inc., Houston, PA.

[16] Sylvester, P. & R. L. Ferrari, 1986, "Finite Elements for Electrical Engineers," Cambridge Univ. Press, New York.

[17] http://www.hephaist.co.jp